

OPEN ACCESS

In Situ Double Probe Beam Deflection Estimating Concentration Profiles of Battery Electrolytes

To cite this article: Katherine Betts *et al* 2025 *J. Electrochem. Soc.* **172** 040521

View the [article online](#) for updates and enhancements.

You may also like

- [The effects of polymer molecular weight on the performance of single-layer polymer light emitting diodes](#)

Mostafa Mergani, Afshin Shahalizad, Sohrab Ahmadi Kandjani *et al.*

- [InGaAs-based planar barrier diode as microwave rectifier](#)

Nor Farhani Zakaria, Shahrir Rizal Kasjoo, Zarimawaty Zailan *et al.*

- [Nondestructive Evaluation of Materials by Photoacoustic Microscope and Photothermal Beam Deflection](#)

Masanobu Kasai, Tsuguo Sawada, Yohichi Gohshi Tomoharu Watanabe *et al.*

ECC-Opto-10 Optical Battery Test Cell: Visualize the Processes Inside Your Battery!

EL-CELL
electrochemical test equipment



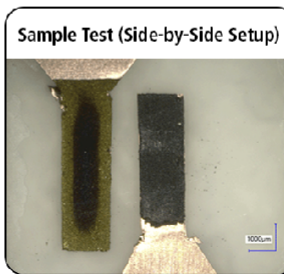
- ✓ **Battery Test Cell for Optical Characterization**
Designed for light microscopy, Raman spectroscopy and XRD.
- ✓ **Optimized, Low Profile Cell Design (Device Height 21.5 mm)**
Low cell height for high compatibility, fits on standard samples stages.
- ✓ **High Cycling Stability and Easy Handling**
Dedicated sample holders for different electrode arrangements included!
- ✓ **Cell Lids with Different Openings and Window Materials Available**



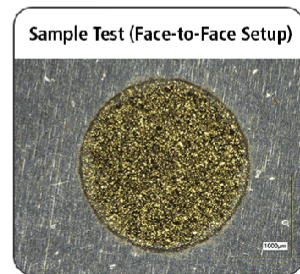
Scan me!

Contact us:

- 📞 +49 40 79012-734
- ✉️ sales@el-cell.com
- 🌐 www.el-cell.com



Sample Test (Side-by-Side Setup)



Sample Test (Face-to-Face Setup)



In Situ Double Probe Beam Deflection Estimating Concentration Profiles of Battery Electrolytes

Katherine Betts,* Michael Frailey, Kidus Yohannes, and Zchange Feng^{*z}

Department of Chemistry and Biochemistry, University of Nevada, Las Vegas, Las Vegas, Nevada 89154, United States of America

An *in situ* double probe beam deflection (PBD) technique has been developed using two laser beams to map the concentration profile of the diffusion layer in an electrochemical cell. A microscale moving upper probe and a fixed position secondary beam offer real-time concentration gradients to be profiled throughout the depth of the diffusion layer. The double PBD technique was used to plot concentration profiles for 0.1 mol kg⁻¹ CuSO₄ and ZnSO₄ within a range of applied currents, showing increased magnitudes of gradients for higher currents. Both single and double beam PBD were explored, demonstrating the distance and time dependence of the developing concentration gradient. While CuSO₄ showed a systematic trend of increased response delay and decreased deflection with increased distance from the electrode, ZnSO₄ experienced some additional phenomena affecting the refractive index within the diffusion layer. The *in situ* double probe beam deflection was shown to be highly sensitive and offers future work in quantifying charge migration within this important region of the electrochemical cell.

© 2025 The Author(s). Published on behalf of The Electrochemical Society by IOP Publishing Limited. This is an open access article distributed under the terms of the Creative Commons Attribution 4.0 License (CC BY, <https://creativecommons.org/licenses/by/4.0/>), which permits unrestricted reuse of the work in any medium, provided the original work is properly cited. [DOI: [10.1149/1945-7111/adca03](https://doi.org/10.1149/1945-7111/adca03)]



Manuscript submitted January 25, 2025; revised manuscript received March 20, 2025. Published April 17, 2025.

The concentration profile within electrochemical cells is particularly important in understanding the transport properties and thermodynamic behavior of battery electrolytes. For improved efficiency and performance of next-generation batteries, research must address uniformity in metal plating, problematic dendrite growth, and mass-transport limitations. A deeper understanding of battery concentration gradients within the diffusion layer offers crucial information to address the limitations in innovative new electrochemical systems.

Measuring Concentration Gradients

Previously explored techniques for profiling concentration gradients include Raman,¹ Infrared,² and NMR³ spectroscopy. These techniques either track concentration change over time at the electrode surface or analyze changes in spectroscopic response spatially between two electrodes with the use of a moveable stage. Although these techniques show potential in battery research, this specialized equipment is expensive and not readily available. Alternatively, optical techniques offer affordable and non-invasive methods to profile concentration gradients across the diffusion layer. Such techniques have been in development since the 1970's, through the measurement of shifted interferogram fringes. Despite complications regarding fringe distortion and boundary reflection effects, interferogram techniques proved successful in measuring both distance and time dependent concentration profiles in electrochemical processes.⁴⁻⁶ Later, Denpo et al. and Fukunaka were able to correct boundary layer distortions and make measurements of profiles sensitive to a 0.01 M concentration change across a 0.5 mm distance from the electrode.^{7,8} Calculated gradients have been accompanied by optical absorbance visualizations.⁹ Miki et al. and Kamesui et al. have more recently used a digital holographic interferometric microscope to measure Li⁺ and Cu²⁺ concentration profiles.^{10,11} Modern digital detectors allow for high spatial resolution, increasing the accuracy of optical techniques. Here we offer an alternative probe beam deflection method which has been shown to estimate concentration gradients of <0.001 M over a distance of 0.2 mm from the electrode surface, showing the opportunity for increased sensitivity. This probe beam deflection is an affordable and non-invasive method to profile concentration gradients across the diffusion layer.

Probe beam deflection (PBD).—The PBD technique tracks the flux of ions close to the electrode surface due to applied potential. The refractive index is concentration-dependent, and with the probe beam path running parallel to the electrode surface we can observe changes in concentration through the beam's corresponding refraction and deflection. When current is applied to the electrochemical cell, a refractive index gradient, $\partial n/\partial x$, is established across the diffusion layer. The relationship between the angle of deflection, θ , and this gradient is described by the following equation.^{12,13}

$$\theta = (L/n_0)(\partial n/\partial x) \quad [1]$$

where L is the length of the electrode surface parallel to the probe beam, and n_0 is the refractive index of the bulk solution. The refractive index gradient and the cell concentration gradient are directly related by:^{12,14}

$$(\partial n/\partial x)_t = (\partial n/\partial c)(\partial c/\partial x)_t = \Psi(\partial c/\partial x) \quad [2]$$

where Ψ is the concentrative refractivity (change in refractive index per unit concentration, mol/kg) measured using a refractometer to find concentration dependent refractive indices. With the electrode at a fixed distance from the position detector, simple geometry (shown in Fig. 1a) allows the conversion of PBD measurements to time dependent angular deflection, θ , and associated concentration gradient. By measuring the concentration gradient at incremental distances from the electrode surface, a concentration profile can be plotted.

In situ double PBD (2-beam).—When a current is applied to an electrochemical cell, the concentration profile changes with time until the steady state is reached, where there is no net movement of ions across the cell. At a steady state, the concentration profile is considered linear, but before this, the depth and shape of the concentration profile are dependent and constantly changing. Plotting a profile using PBD requires multiple data points (and associated measurements) across the depth of the diffusion layer, and we must be sure that the cell is behaving uniformly with each measurement to be able to combine data into a single profile. To ensure consistency of the cell response, a second PBD beam is introduced at a fixed reference point from the electrode surface as shown in Fig. 1b. As this beam remains fixed throughout multiple measurements, it should respond uniformly, giving a reference point for the edge of the diffusion layer. The concentration gradients measured are evolving with time, and the data collected describes a

*Electrochemical Society Member.
zE-mail: zchange.feng@unlv.edu

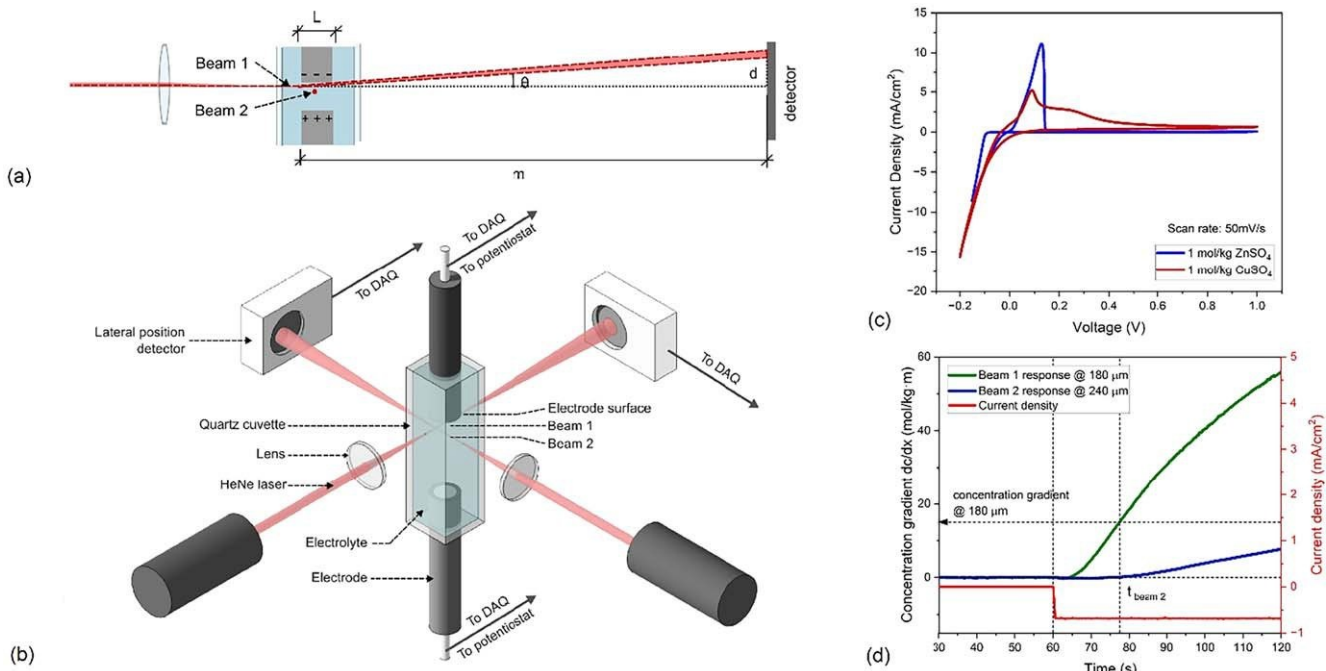


Figure 1. Experimental setup. (a) Probe beam deflection geometry, (b) in situ double probe beam deflection apparatus schematic, (c) cyclic voltammograms for 1 mol kg⁻¹ CuSO₄ and 1 mol kg⁻¹ ZnSO₄, scan rate 50 mV s⁻¹, (d) example concentration gradient measurement taken at 180 μ m from the electrode surface, -0.71 mA cm⁻² applied current density, 0.1 mol kg⁻¹ CuSO₄, demonstrating the in situ nature of the two beam technique.

moment in time corresponding to a chosen depth of diffusion layer. Each data point for a single concentration gradient is taken at a time where the diffusion layer has evolved to reach Beam 2, at a fixed distance from the electrode surface. The initial deflection response of Beam 2 can be used as a time reference to find the corresponding concentration gradient data point from Beam 1, as demonstrated in Fig. 1d. This ensures the in situ nature of the overall measurement from a single experiment. A single beam PBD method as discussed below is also effective but relies on separate measurements to gain one gradient data point, and, therefore, we consider the double PBD method superior. This method allows in situ coordinated data collection for the gradient at multiple distances from the electrode, as well as a boundary for the edge of the diffusion layer where concentration can be considered that of the bulk, c_0 .

Single PBD (1-beam).—Another way to consider the concentration profile assumes uniformity in cell behavior and uses a single PBD beam to take measurements at multiple distances from the electrode surface. Any one of the measurements can be used as the boundary to the diffusion layer, where the concentration is considered that of the bulk, c_0 , at time, t . Concentration gradients, $\partial c/\partial x$, for those measurements taken closer to the electrode, are all recorded at time t , giving a single time-dependent concentration profile.

Method

Each PBD system consisted of a 633 nm HeNe laser (ThorLabs HRS015B, Newport N-STM-912), a 100 mm lens to focus the beam to 150 μ m, and a photodiode-based lateral position detector (ThorLabs PDP90A) connected to a multi-channel data acquisition system. The two beams were arranged one above the other at 90° to each other, with Beam 1 position set with its outer edge at the electrode surface ($x \approx 80 \mu$ m, beam center) and Beam 2 outer edge set at 200–240 μ m, depending on the applied current and associated sensitivity. The electrochemical cell was positioned at the lens focal point and consisted of a 10 mm quartz cuvette containing two 3 mm electrodes (glassy carbon WE, copper/zinc CRE) spaced 5 mm apart. The electrochemical cell was filled with 0.1 mol kg⁻¹ CuSO₄ (Sigma-Aldrich) or 0.1 mol kg⁻¹ ZnSO₄ (J.T. Baker), argon purged

for 20 min, and passed through 5 cyclic voltammogram cleaning cycles (100 mV s⁻¹) before resting to equilibrium.

To run each PBD experiment, measurements were first taken with Beam 1 at $x = 80 \mu$ m, by monitoring beam position at equilibrium for >1 min, then applying a 1 min, -0.71 mA cm⁻² pulse to the electrochemical cell using a potentiostat (Biologic SP300) and allowing 15 min of rest time for the cell to return to equilibrium. Positive current was passed between measurements to remove deposited metal at the electrode surface and the system was again rested to equilibrium. The Beam 1 laser and lens were moved downwards 20 μ m using a micro-scale transition stage before the next measurement was taken, leaving beam 2 in a fixed position for reference. Measurements were taken at 20 μ m increments until a position set to 20 μ m above the outer edge of Beam 2. PBD experiments were carried out at -0.71 mA cm⁻², -0.35 mA cm⁻², and -0.14 mA cm⁻² (by applying -50 μ A, -25 μ A, and -10 μ A respectively to a 3 mm diameter electrode), for solutions of 0.1 mol kg⁻¹ CuSO₄ and 0.1 mol kg⁻¹ ZnSO₄.

With the potentiostat and position detectors both connected to the data acquisition system, the time response of the PBD was captured, and the time response of reference Beam 2 was used to find the corresponding concentration gradient, $\partial c/\partial x$, from Beam 1. Starting from the known initial concentration of the solution, c_0 , the measured gradients were used to calculate the concentration at each Beam 1 position, e.g., if c_0 is set at 240 μ m, the gradient measured by Beam 1 at 220 μ m is considered as the average slope from 220 μ m to 240 μ m and is used to calculate the concentration at 220 μ m. Using PBD, solution density, and refractive index measurements (Abe refractometer), the concentration gradient through the diffusion layer was plotted using Origin.

Results

Cyclic voltammograms (CVs), taken using the PBD electrochemical cell, for 1 mol kg⁻¹ CuSO₄ (red curve) and 1 mol kg⁻¹ ZnSO₄ (blue curve) are displayed in Fig. 1b. A negative current allowing for copper deposition was observed from -0.05 V (vs Cu/Cu⁺), with an oxidation peak at 0.37 V causing metal stripping. The ZnSO₄ solution showed a cathodic current from 0.00 V (vs Zn/Zn⁺) and an oxidation peak at

0.78 V. The current density range chosen for the PBD measurements (-0.14 mA cm^{-2} , -0.35 mA cm^{-2} , -0.71 mA cm^{-2}), allows for observations relating to ion reduction while avoiding thermal effects due to the temperature dependence of the refractive index.

Figure 1d shows an example of an in situ double PBD gradient measurement, taken at -0.71 mA cm^{-2} in $0.1 \text{ mol kg}^{-1} \text{ CuSO}_4$. For each position from the electrode surface (180 μm position shown), two beam deflections are recorded in unison. Beam 2 (blue curve) responds to the applied current 17.5 s after the -0.71 mA cm^{-2} is applied. At this time ($t_{\text{beam 2}}$) the deflection in Beam 1 (green curve), converted to concentration gradient using Eqs. 1 and 2, is measured to be $15 \text{ mol kg}^{-1}\text{m}$. This gradient contributes the slope leading to 180 μm , from the previous measurement, for the final concentration profile. Each measurement, with Beam 1 at a different distance from the electrode, contributes another slope within the gradient, leading from the bulk concentration at the stationary Beam 2 position.

In situ double PBD results for $0.1 \text{ mol kg}^{-1} \text{ CuSO}_4$ are displayed in Fig. 2. The upper panels show the deflection (in mm) of the height adjustable probe (Beam 1) from 80 μm (black curve, largest deflection), out toward the bulk solution. With each 20 μm increment, the deflection reduces in magnitude (black through yellow curves) and there is a delay in the response proportional to the gradient's spread from the electrode surface. The lower panels of Fig. 2a, b, c show a consistent response from the stationary Beam 2. When cathodic current is applied to the electrochemical cell (green curve), the potential drops from open circuit potential (blue curve) as the concentration of the electrolyte at the electrode surface decreases due to ion consumption during metal plating. This decreased concentration is lower in refractive index than the bulk electrolyte and causes the probe to deflect in the direction of the electrode surface. The change in lateral position grows with the concentration gradient as current is applied, followed by relaxation of the gradient, beam deflection and potential.

As the applied current is increased, a larger deflection is recorded, and a steeper concentration profile is observed. Measured concentration

profiles for -0.14 mA cm^{-2} , -0.35 mA cm^{-2} , and -0.71 mA cm^{-2} can be seen in Figs. 2(d)–2(f) respectively. The gradient between data points in the concentration profile is taken from the corresponding Beam 1 measurement, at the time at which Beam 2 responds to the applied current. As can be seen in the distance-dependent shape of the deflection, the gradient/slope decreases in magnitude as it reaches the outer region of the diffusion layer. The concentration profile of the diffusion layer is often depicted and modeled as a linear slope reaching out to the bulk at c_0 , but the PBD measurements show a polynomial relationship with a curved transition into the bulk electrolyte. All polynomial (x^3) curve fitting demonstrates $R^2 > 0.99$.

Single PBD measurements for $0.1 \text{ mol kg}^{-1} \text{ ZnSO}_4$ are shown in Fig. 3. The decline in deflection slope and associated concentration gradient with distance from the electrode surface is demonstrated in 20 μm increments and shown in Figs. 3a–3c. Time-dependent measurements are taken at the time of response from the outermost beam positions (e.g., the probe at 220 μm in Fig. 3c responds at 4.8 s). Gradients used to plot the single beam concentration profiles are all taken at this exact response time. The time-dependent concentration profiles taken at the three outermost beam positions (response time indicated with a dashed line in upper panel) can be seen in Figs. 3d–3f. As time increases, more electrolyte ions are consumed, and the concentration gradient grows. With this differential in concentration, diffusion causes the concentration gradient to spread deeper into the bulk as can be seen by the deeper profile as the system moves toward a steady state. The three time-dependent gradients shown for each applied current demonstrate the increasing slope/gradient with increased time (green curve through purple), reaching a lower surface concentration at the electrode surface. The changing depth of the gradient can also be observed, e.g., the later 4.8 s gradient pushes deeper into the cell than the green 2.0 s curve. All polynomial (x^3) curve fitting demonstrates $R^2 > 0.99$.

For comparison, in situ double PBD and single PBD measurements for $0.1 \text{ mol kg}^{-1} \text{ ZnSO}_4$ are displayed in Figs. 4 and 5 respectively. Beam 2 (with fixed position) remains uniform in its

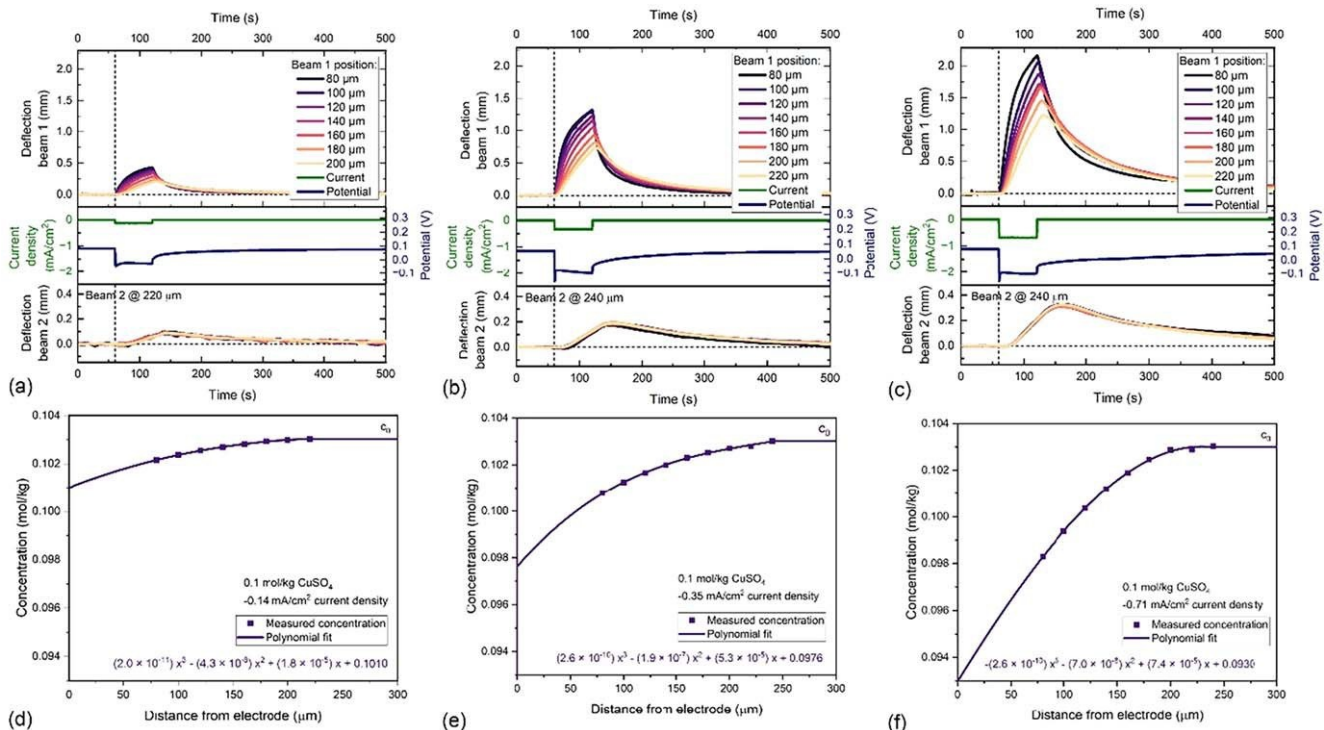


Figure 2. In situ double beam deflections for $0.1 \text{ mol kg}^{-1} \text{ CuSO}_4$. Deflection profiles for Beam 1 at incremental distances from the electrode surface are shown in the upper panels. Deflections for fixed position Beam 2 are shown in the lower panels for (a) -0.14 mA cm^{-2} (b) -0.35 mA cm^{-2} , (c) -0.71 mA cm^{-2} applied current density. Calculated concentration gradients using the time response from Beam 2 at (d) -0.14 mA cm^{-2} , (e) -0.35 mA cm^{-2} , (f) -0.71 mA cm^{-2} applied current density.

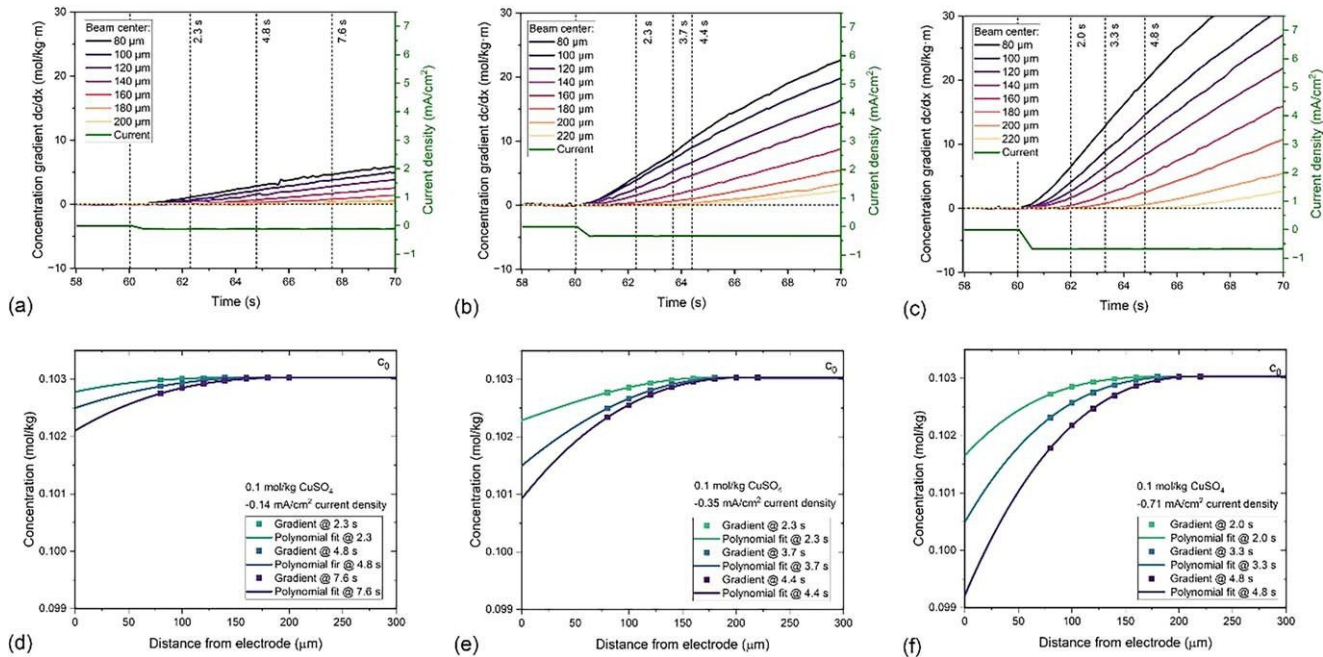


Figure 3. Time dependent concentration gradient measurements, $\partial C / \partial x$, for single beam deflections using $0.1 \text{ mol kg}^{-1} \text{ CuSO}_4$. Gradients shown at incremental distances from the electrode surface for (a) -0.14 mA cm^{-2} (b) -0.35 mA cm^{-2} , (c) -0.71 mA cm^{-2} applied current density. Corresponding concentration gradients using single beam deflection data at (d) 0.14 mA cm^{-2} , (e) -0.35 mA cm^{-2} , (f) -0.71 mA cm^{-2} applied current density.

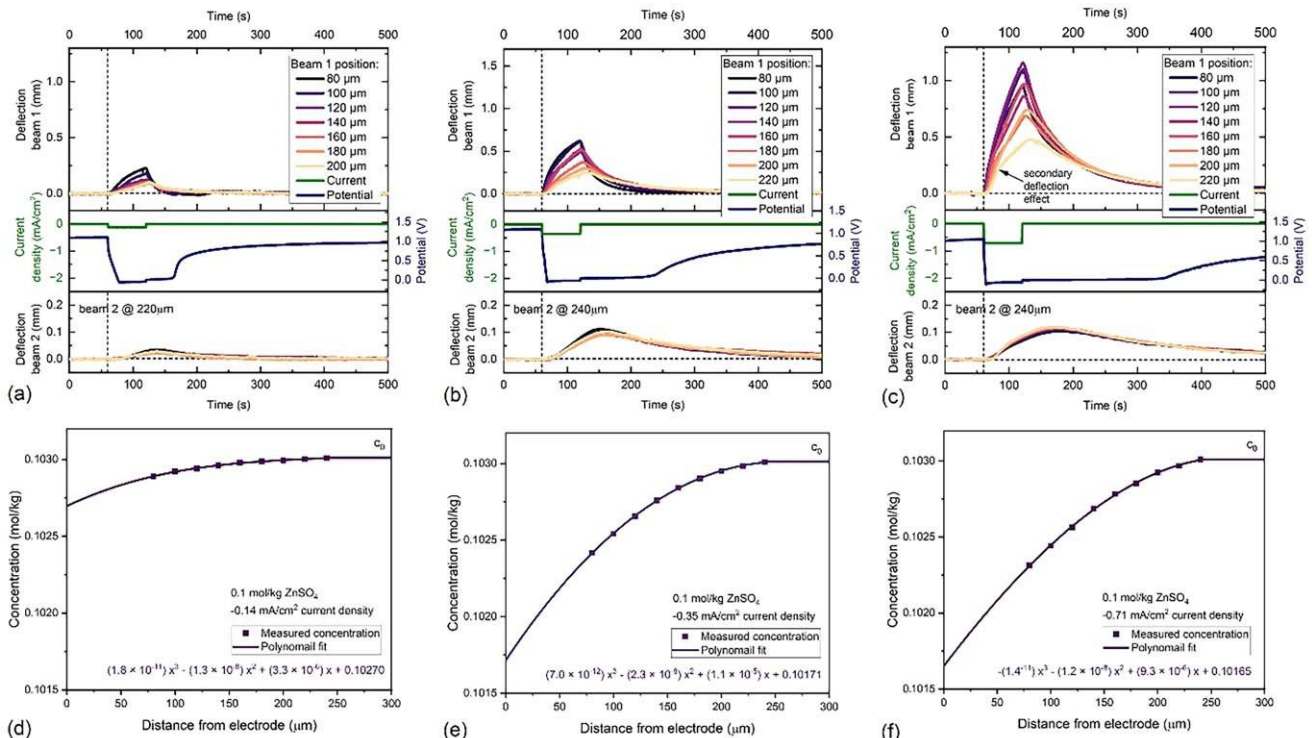


Figure 4. In situ double beam deflections for $0.1 \text{ mol kg}^{-1} \text{ ZnSO}_4$. Deflection profiles for Beam 1 at incremental distances from the electrode surface are shown in the upper panels. Deflections for fixed position Beam 2 are shown in the lower panels for (a) -0.14 mA cm^{-2} (b) -0.35 mA cm^{-2} , (c) -0.71 mA cm^{-2} applied current density. Calculated concentration gradients using the time response from Beam 2 at (d) -0.14 mA cm^{-2} , (e) -0.35 mA cm^{-2} , (f) -0.71 mA cm^{-2} applied current density.

response, while Beam 1 is moved away from the electrode surface, demonstrating a decrease in gradient with each 20 μm . The corresponding concentration profiles become steeper with increased applied current, and all polynomial (x^3) curve fitting demonstrates $R^2 > 0.99$. The ZnSO_4 PBD showed smaller maximum deflection

compared with CuSO_4 , forming concentration gradients smaller in magnitude, which may be due to the differences in the transference number between the two salts. There is also a notable change in the trend for distance dependent deflection for the applied current in ZnSO_4 . Figure 5c shows the probe initially deflecting as expected

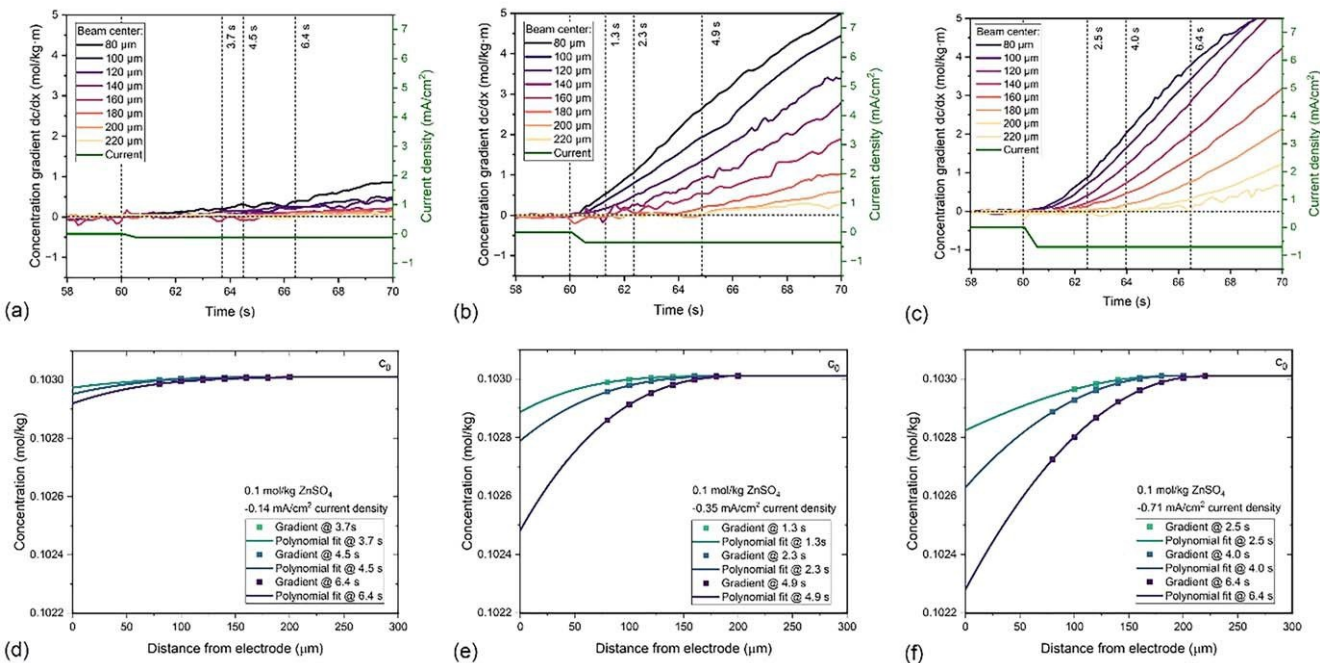


Figure 5. Time dependent concentration gradient measurements, $\partial c / \partial x$, for single beam deflections using $0.1 \text{ mol kg}^{-1} \text{ ZnSO}_4$. Gradients shown at incremental distances from the electrode surface for (a) -0.14 mA cm^{-2} (b) -0.35 mA cm^{-2} , (c) -0.71 mA cm^{-2} applied current density. Corresponding concentration gradients using single beam deflection data at (d) 0.14 mA cm^{-2} , (e) -0.35 mA cm^{-2} , (f) -0.71 mA cm^{-2} applied current density.

(probes further from the electrode surface deflect less), but Fig. 4c shows a secondary change in deflection, showing an inconsistent bend in the deflection peak profile. Despite repeat trials, this phenomenon was continued. Due to the low reduction potential of zinc metal, it is possible that parasitic side reactions with water at the electrode cause surface disturbances which impact the concentration gradient measurements. Hydrogen evolution reaction, and associated coordination with OH^- and Zn^{+} ions can affect the efficiency of transport and the forming concentration gradient.^{15,16}

Discussion

The in situ double PBD technique demonstrated the relationship between deflection response and distance from the electrode surface for an operating electrochemical cell. Once a cathodic current is applied to the system and reactants are consumed, a concentration gradient emerges from the electrode out to the bulk electrolyte. The plotted concentration profile, the timing of its emergence, and the associated charge transfer are dependent on the transport properties of the studied electrolyte. Optical beam deflection techniques have previously been used to study the variation of diffusion with concentration,¹⁷ and quantify the diffusion coefficient of battery electrolytes.^{18,19} With precise plotting of time-dependent concentration profiles, it may also be possible to quantify other transport properties such as transference numbers using the double PBD technique.

The difference in the scale of deflection for the CuSO_4 and ZnSO_4 solutions, and the impact on measurements for other electrolytes should be further investigated. For example, the concentration gradients recorded due to -0.71 mA cm^{-2} applied current reached $20 \text{ mol kg}^{-1} \cdot \text{m}$ within 5 s for CuSO_4 (refer to Fig. 3c), while the ZnSO_4 reached $3 \text{ mol kg}^{-1} \cdot \text{m}$ (refer to Fig. 5c). A computational model of the in situ double PBD system will contribute to future work, in order to quantify errors associated with differences in transference number and refractive index while considering other factors such as hydrogen evolution reaction (HER). Despite the varying scale of deflection, the method was

shown to be highly sensitive, with the stationary Beam 2 recording maximum deflections of $0.031 \pm 0.005 \text{ mm}$ (average of 7 measurements) for -0.14 mA cm^{-2} applied to the ZnSO_4 electrolyte. The small deviation between measurements not only demonstrates the sensitivity of the method but also addresses confidence in applying multiple Beam 1 measurements to form one concentration profile. This confidence is at the core of the in situ double beam approach to PBD.

Despite the successful qualitative result of this PBD study, the quantitative aspect of the experimental setup was challenging due to the microscale of the measurements combined with the $150 \mu\text{m}$ beam diameter of the laser beams. Not only does a large beam limit how close the probe can get to the electrode surface, but it also limits the distance between the electrochemical cell and the position detector, due to the divergence of the beam and the maximum spot size the sensor can accurately detect (9 mm max.). Rudnicki et al. discuss the effect of probe diameter with respect to the Gaussian intensity profile of the beam.²⁰ For accurate quantitative measurements and modeling, the differential section of the beam must be considered, along with varied deflection dependent on its position within the concentration gradient and power density of the probe. The initial beam position is set by finding the upper-most region in which the beam achieves maximum intensity at the position sensor, without obstruction or distortion by the electrode. This outer edge of the probe beam accounts for a larger diameter ($240 \mu\text{m}$) than the conventionally calculated beam diameter ($d_{1/e^2} = 150 \mu\text{m}$) and includes intensity $<5\%$ of the centerline intensity.²⁰ Previous PBD studies have offered beam diameters of $50\text{--}216 \mu\text{m}$,^{12,14,20} and while the presented probe is within this range, there is some error associated with the Gaussian nature of the beam and the initial probe offset. Future work will focus on reducing the beam waist size while ensuring the associated Rayleigh range allows for uniformity of the probe across the electrode length, L .

The effects of induced convection due to the density difference across the diffusion layer should be considered. By limiting the applied current, we induce a very small concentration (and density) gradient, minimizing any associated error. The applied current

density of -0.14 mA cm^{-2} induced a concentration gradient of $< 0.001 \text{ M}$. Through fine-tuning of electrode diameter, beam size, and position calibration, the PBD experiment can move towards a more quantitative measurement of the diffusion layer and associated transference of charge.

Conclusions

The results for the in situ double and single PBD showed a consistent trend/shape for distance dependent deflection, offering emerging concentration gradient values at small increments from the electrode surface. The fixed position of a secondary beam demonstrated uniformity between electrochemical cell behavior and offered in situ correlated measurements between the edge of the diffusion layer and the concentration gradient at Beam 1. In-situ double PBD measurements allowed real-time concentration gradients to be calculated throughout the depth of the diffusion layer, converting lateral deflection into measured concentration gradients, $\partial c/\partial x$, which were used to plot concentration profiles for $0.1 \text{ mol kg}^{-1} \text{ CuSO}_4$ and ZnSO_4 . The slope/scale of the gradient was shown to be dependent on both time and the magnitude of the applied current, and the measurements consistently produced a polynomial (x^3) fit, describing a diffusion layer that curves at the junction with bulk concentration, c_0 , but appears relatively linear as it reaches the electrode surface.

Future work will reduce the beam size, allowing measurements at closer proximity to the electrode surface, and greater sensitivity by offering more distance to the position detector. Computational modeling will also be explored, accounting for the spatial resolution associated with the Gaussian intensity profile of the probe, as well as the impact of different electrolyte systems and their transport properties. With these improvements, there will be a focus on quantitative measurements of transferred charge which will contribute important information regarding the battery diffusion layer. The in situ double PBD technique offers a highly sensitive, broadly available solution for a deeper understanding of novel electrolyte systems and their concentration profiles.

Acknowledgments

This work is supported by a grant from NSF (CBET-2243098). Kidus Yohannes would thank the financial support from an NSF grant (OIA-2225755).

ORCID

Katherine Betts  <https://orcid.org/0009-0004-7412-1806>
Zhang Feng  <https://orcid.org/0009-0006-5664-531X>

References

1. J. Fawdon, J. Ihli, F. L. Mantia, and M. Pasta, *Nat. Commun.*, 12, 4053 (2021).
2. A. David, M. Silverman, K. Kim, and D. J. Hallinan, *J. Phys. Chem. B*, 127, 9587 (2023).
3. A. K. Sethurajan, S. A. Krachkovskiy, I. C. Halalay, G. R. Goward, and B. Protas, *J. Phys. Chem. B*, 119, 12238 (2015).
4. F. R. McLarnon, R. H. Muller, and C. W. Tobias, *J. Opt. Soc. Am., JOSA*, 65, 1011 (1975).
5. R. H. Muller, *Electrochim. Acta*, 22, 951 (1977).
6. Y. Fukunaka, K. Denpo, M. Iwata, K. Maruoka, and Y. Kondo, *J. Electrochem. Soc.*, 130, 2492 (1983).
7. K. Denpo, T. Okumura, Y. Fukunaka, and Y. Kondo, *J. Electrochem. Soc.*, 132, 1145 (1985).
8. Y. Fukunaka, Y. Nakamura, and Y. Konishi, *J. Electrochem. Soc.*, 145, 3814 (1998).
9. M. Rosso, Y. Huttel, E. Chassaing, B. Sapoval, and R. Gutfraind, *J. Electrochem. Soc.*, 144, 1713 (1997).
10. A. Miki et al., *J. Mater. Chem. A*, 9, 14700 (2021).
11. G. Kamesui, K. Nishikawa, H. Matsushima, and M. Ueda, *J. Electrochem. Soc.*, 168, 031507 (2021).
12. J. Pawliszyn, M. F. Weber, M. J. Dignam, and S. Moon. Park, *Anal. Chem.*, 58, 239 (1986).
13. E. D. Bidoia, F. McLarnon, and E. J. Cairns, *J. Electroanal. Chem.*, 482, 75 (2000).
14. C. A. Barbero, *Phys. Chem. Chem. Phys.*, 7, 1885 (2005).
15. H. Yan, S. Li, J. Zhong, and B. Li, *Nano-Micro Lett.*, 16, 15 (2023).
16. X. Luo, W. Peng, Y. Li, F. Zhang, and X. Fan, *Green Energy & Environment*, 7, 858 (2022).
17. A. Kurian et al., *Pramana - J. Phys.*, 43, 401 (1994).
18. K. Betts et al., *J. Electrochem. Soc.*, 171, 020551 (2024).
19. C. Barbero, M. C. Miras, R. Kötz, and O. Haas, *Solid State Ionics*, 60, 167 (1993).
20. J. D. Rudnicki et al., *J. Electroanal. Chem.*, 362, 55 (1993).